**Supplementary figure legends**

### Fig. S1. Localization of EB3 during each stage of mitosis.

HeLa cells that stably expressed GFP-EB3 were fixed with methanol at -20°C for 1 min, washed twice with PBS, and then permeabilized for 5 min in PBS containing 0.2% Triton X-100. Immunofluorescence staining was performed as described in "Materials and methods". Green, GFP-EB3; red, α-tubulin; blue, DAPI.

### Fig. S2. The specificity of the anti-phospho-EB3(Ser176) polyclonal and monoclonal antibodies.

(**A**) Phospho-specific EB3 Ser176 polyclonal and monoclonal antibodies recognize *in vitro* phosphorylated EB3 by Aurora-B. GST-fused EB3 was incubated with Glu-Glu-Aurora-B in the presence or absence of cold ATP. The phosphorylation reactions were detected by western blots probed sequentially with anti-phospho-EB3(Ser176) rabbit polyclonal (upper left panel), anti-phospho-EB3(Ser176) monoclonal (left lower panel) and anti-EB3 (right panels) antibodies. (**B**) Examination of the specificity of the anti-phospho-EB3(Ser176) monoclonal antibody 9.7.5 by immunofluorescence study. HeLa cells that stably expressed GFP-EB3 were treated with siRNA of EB3 for 48 hr, and then immunofluorescence staining was performed. Green, GFP-EB3; red, phospho-EB3(Ser176); blue, DAPI. Arrows indicate EB3 knockdown mitotic cells. Arrowheads point to cells that were not transfected with EB3 siRNA at the corresponding cell cycle phase. (**C**) Effects of Aurora knockdown on EB3 phosphorylation. HeLa cells that stably expressed GFP-EB3 were treated with siRNAs for Aurora-A or Aurora-B for 48 hr, and then immunofluorescence staining was performed. Representative confocal images of three independent experiments are shown. Red, phospho-EB3(Ser176); green, GFP-EB3; blue, DAPI. Left panel, metaphase cell; right panel, telophase cell.

### Fig. S3. Proteasomal degradation of endogenous EB3.

Western blots with anti-EB3 antibody using HeLa cell lysates treated with 10 μg/ml cycloheximide (CHX) for the indicated times in the presence or absence of 20 μM MG132.

### Fig. S4. SIAH-1 does not promote ubiquitination of EB1 and EB2.

(**A**) SIAH-1 interacts with all three EB1 family members *in vitro* (top panel). Purified His-EB1, EB2 or EB3 was incubated with GST alone or GST-fused SIAH-1 trapped on glutathione-Sepharose beads. Then, bound His-tagged protein was eluted and detected by western blots with anti-penta-His antibody. The bottom panel shows Ponceau staining of the GST fusion protein samples used in the assay. (**B**) SIAH-1–mediated *in vitro* ubiquitination of EB3, but not of EB1 nor EB2, using the system

described in "Materials and methods" (top panel). The bottom panel shows Ponceau staining of the GST fusion protein samples used in the assay. (**C**) SIAH-1–mediated EB3 ubiquitination in cells. HeLa cells were transfected with the indicated plasmids. After 24 hr, cells were treated with 20 μM MG132 for 6 hr. His-Ubiquitin conjugates were recovered on Ni-NTA beads and subjected to western blots using anti-GST antibody.

**Fig. S5. Effects of SIAH-1 knockdown on EB3 protein level.**

HeLa cells were treated with siRNAs for SIAH-1 for 48 hr, and then the cell lysates were subjected to western blots with the indicated antibodies. One western blot shown is representative of two independent experiments.

**Fig. S6. Effects of Aurora phosphorylation on SIAH-1–mediated *in vitro* EB3 ubiquitination.**

GST-fused wild-type EB3 or EB3 S176A was first *in vitro* phosphorylated with His-tagged bacterially purified Aurora-A in the presence of cold ATP, and then *in vitro* ubiquitination assays were performed as described in "Materials and methods".

**Fig. S7. Effects of EB3 knockdown on mitotic progression.**

HeLa cells were treated with siRNAs for EB1 and/or EB3. After 72 hr, morphology of interphase nuclei was determined. (left panels) Patterns of nuclear morphology. Green, α-tubulin; blue, DAPI. (right panel) The rate of total abnormal nuclei (multinuclear, heteromorphic, and micronucleus) was calculated (n = 1000).

**Fig. S8. The binding site of EB3 on the surface of the catalytic domain of SIAH-1.**

(left panel) A surface representation of SIAH-1, colored according to electrostatic potential (negative and positive in red and blue, respectively). (right panel) SIAH-1 is shown in light blue ribbon representation, with β-strands drawn as arrows. The peptide derived from EB3 is shown in dark blue, lying in an extended conformation, and forming hydrophobic interactions with SIAH-l mainly through Val 178 and Pro 180. Ser 176 of EB3 lies close to Met 180 of SIAH-1; its γ-hydroxyl oxygen is located less than 4.0 Å from the sulfur atom.

**Fig. S9. Phosphorylatable residues within the SIAH-binding motifs.**

Alignment of SIAH-binding motifs of various proteins. The sequence Pro-X-Ala-X-Val-X-Pro with Val-X-Pro constituting the core residues is red. Phosphorylatable residues are blue.

**Fig. S10. EB1 family proteins can not activate Aurora-B.**

HeLa cells were transfected with the indicated plasmids. The cell lysates were analyzed by western blots probed sequentially with anti-phospho-Aurora-B, anti-FLAG and anti-myc antibodies.

## Supplementary Fig.1

Ban et al.

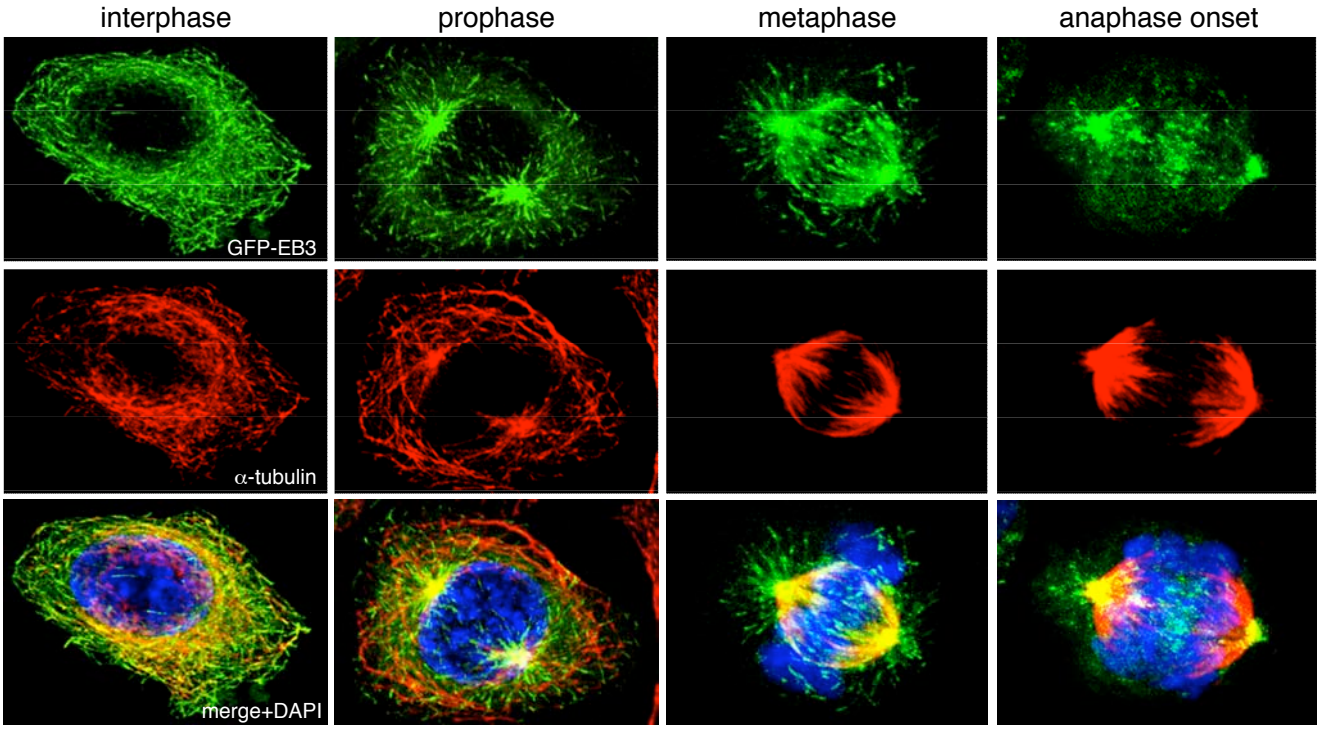


## Supplementary Fig.1 (continued)

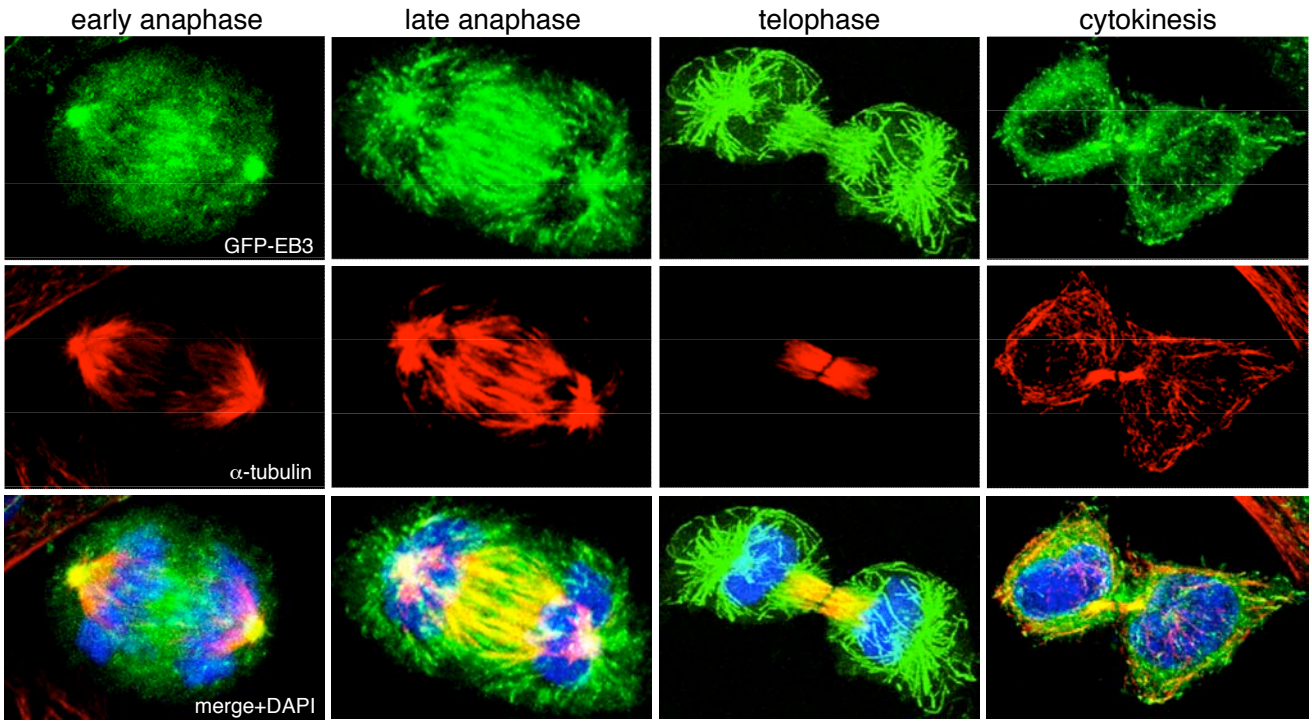

## Supplementary Fig.2A

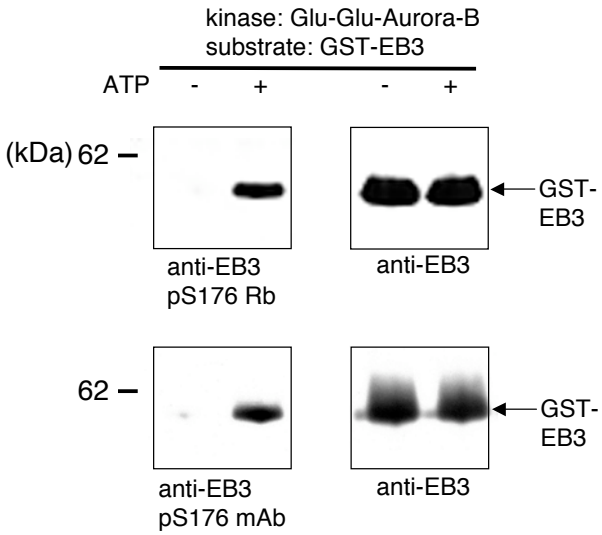


## Supplementary Fig.2B

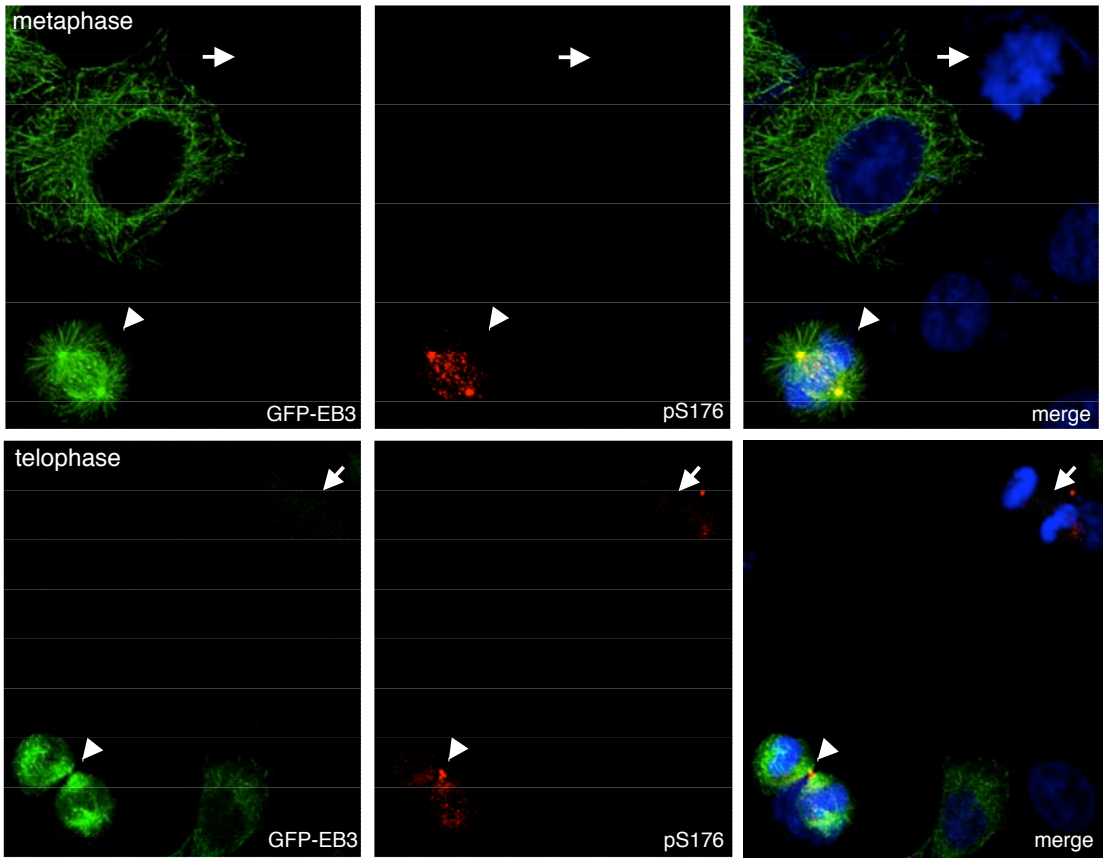

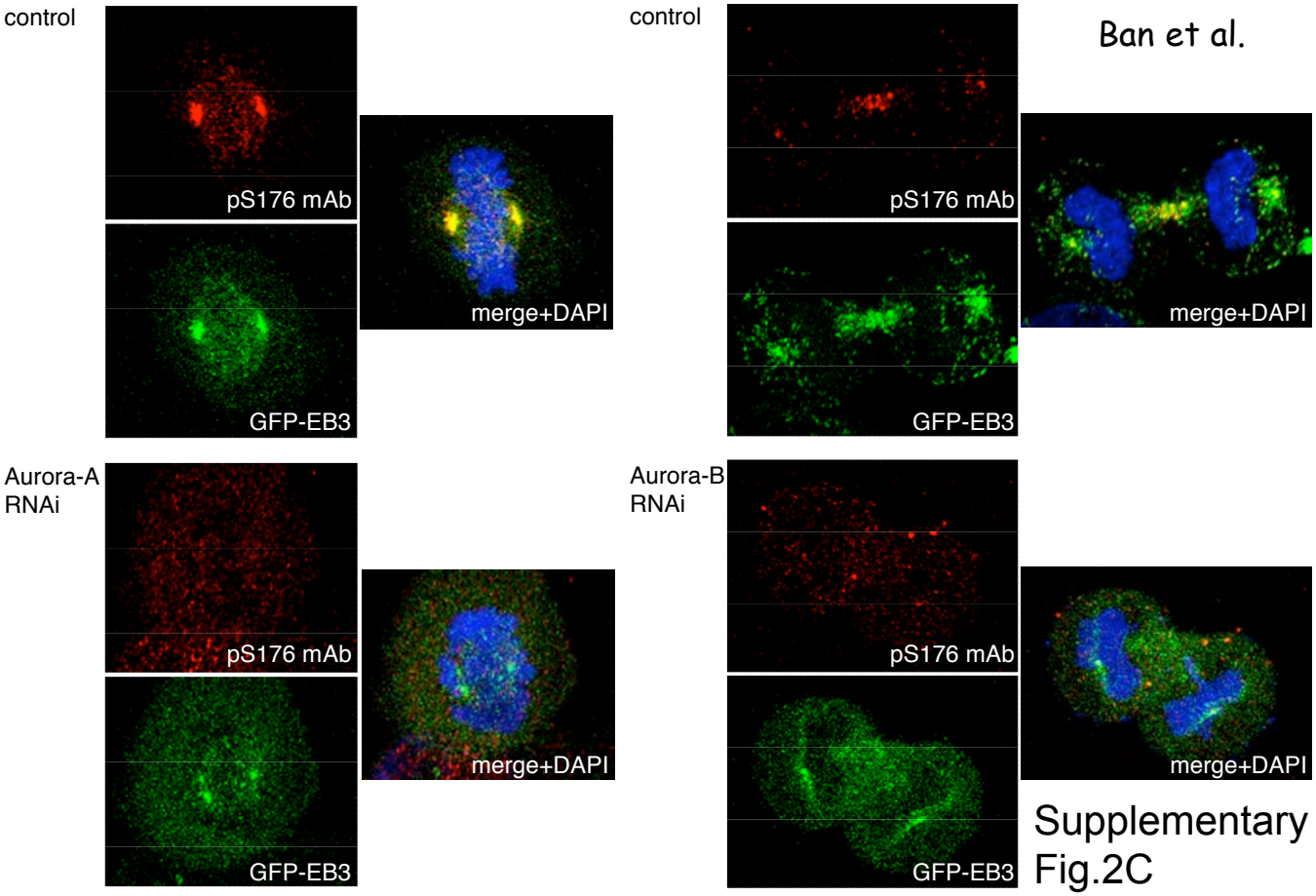


Supplementary Fig.2C

## Supplementary Fig.3

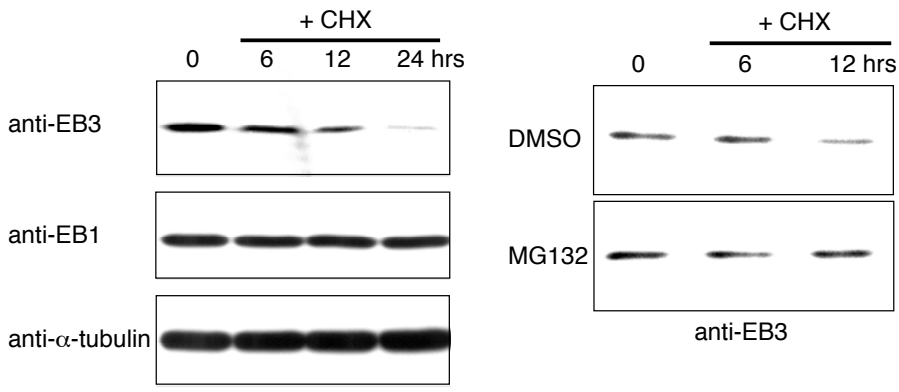

## Supplementary Fig.4A

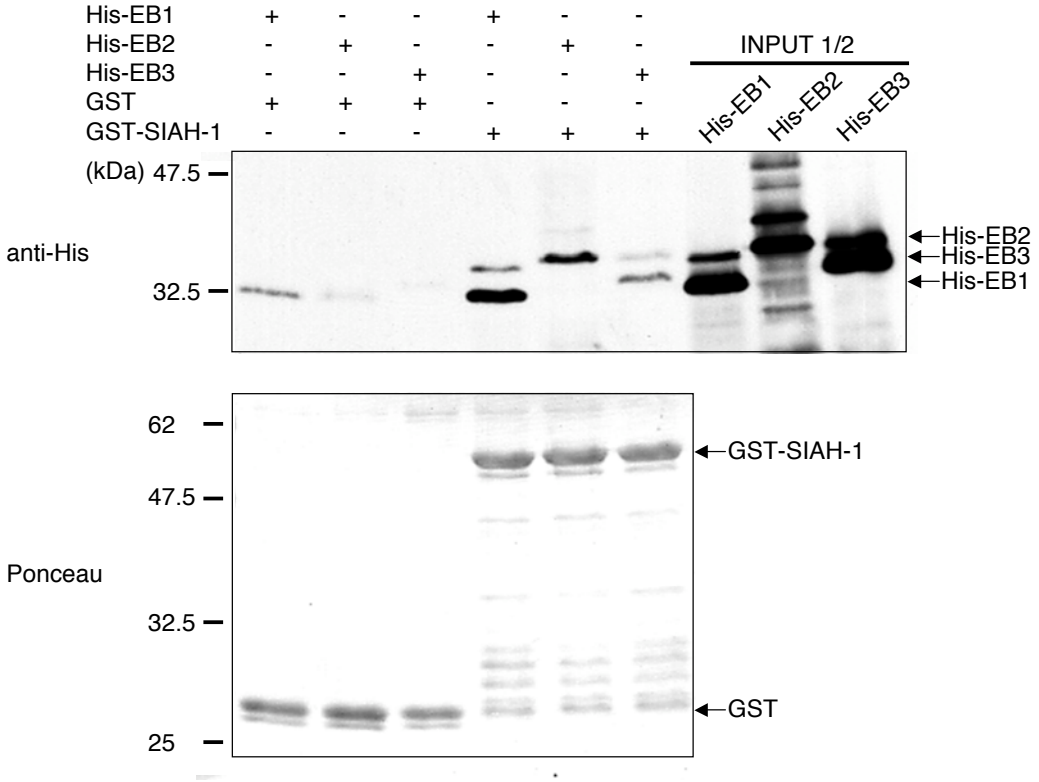


## Supplementary Fig.4B

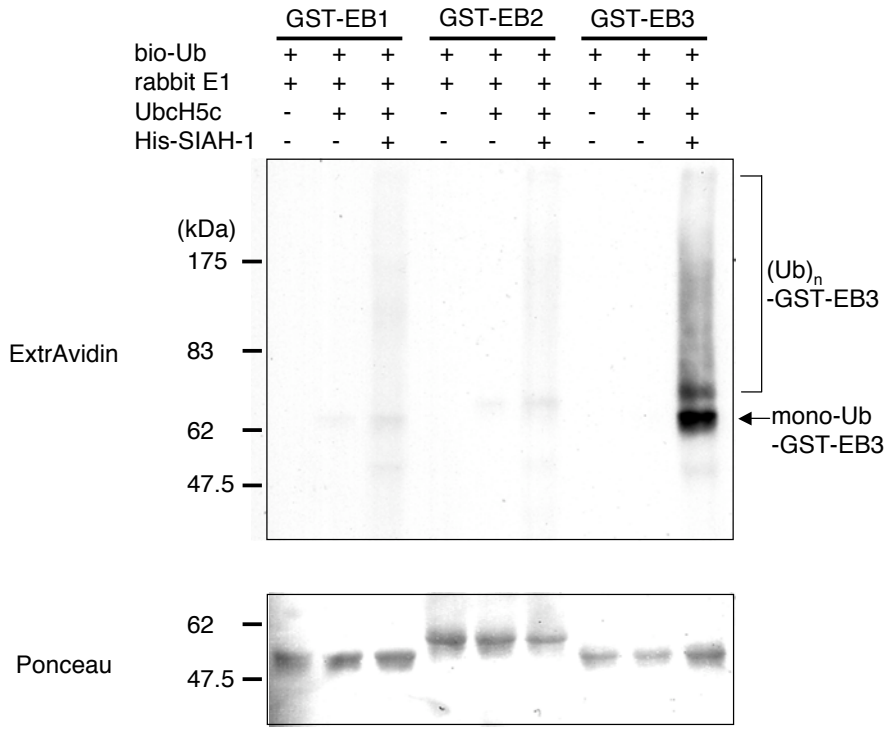

## Supplementary Fig.4C

Ban et al.

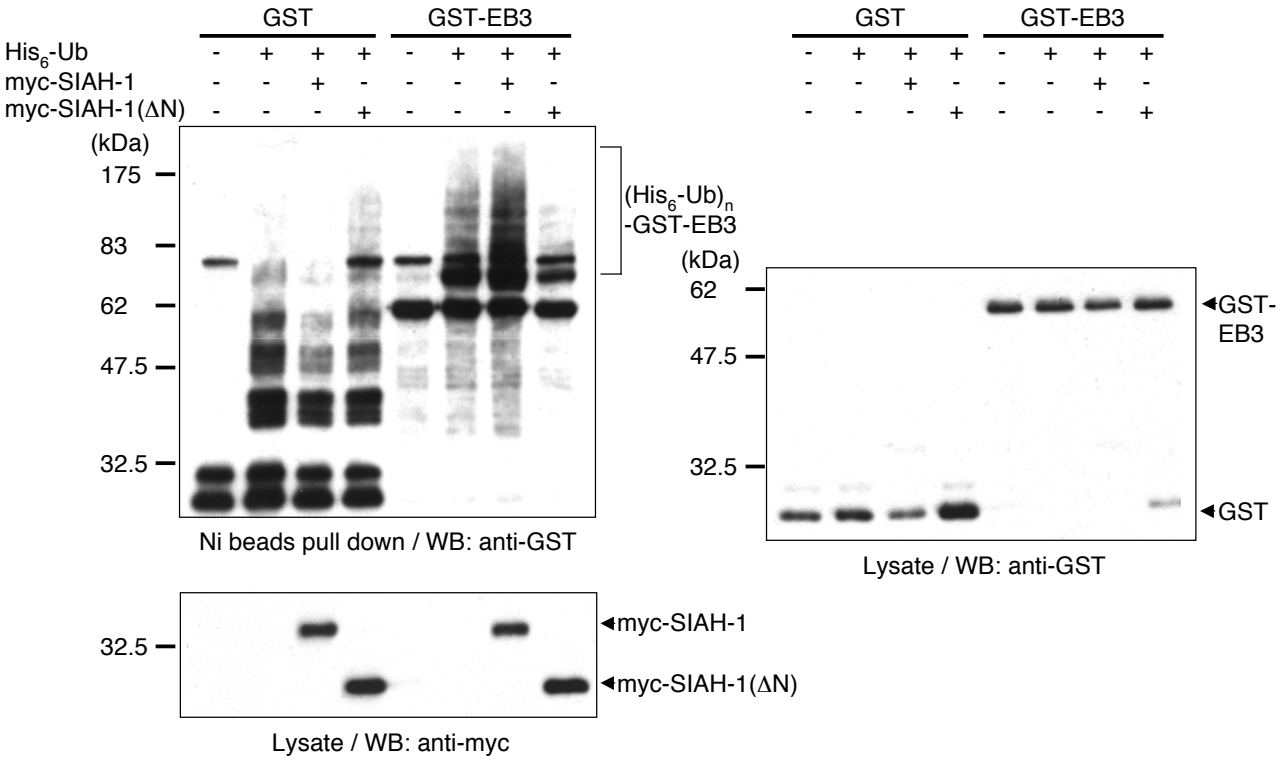


## Supplementary Fig.5

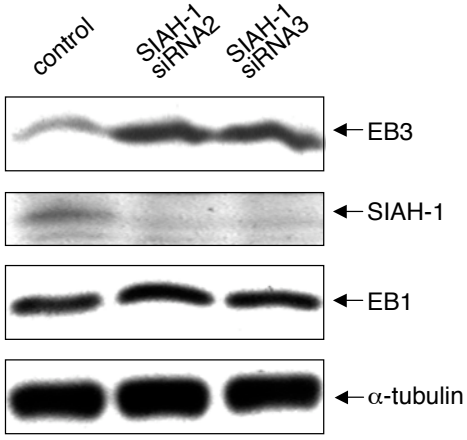

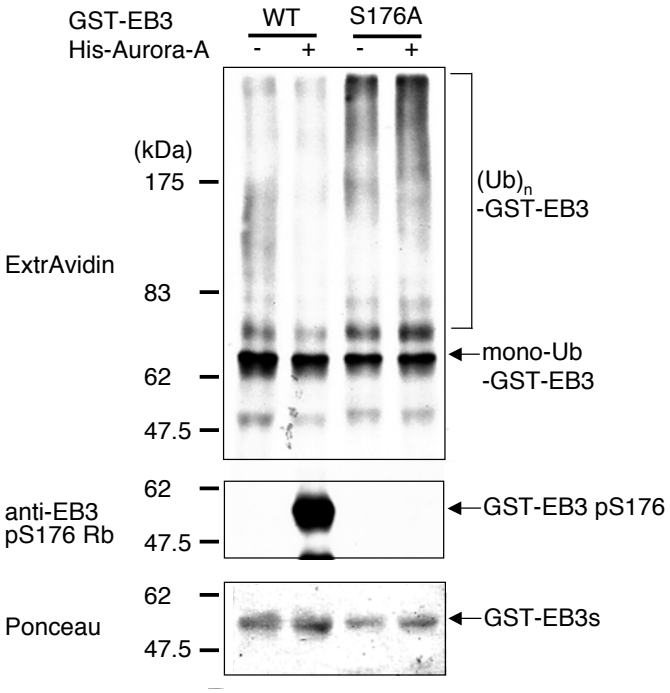


## Supplementary Fig.7

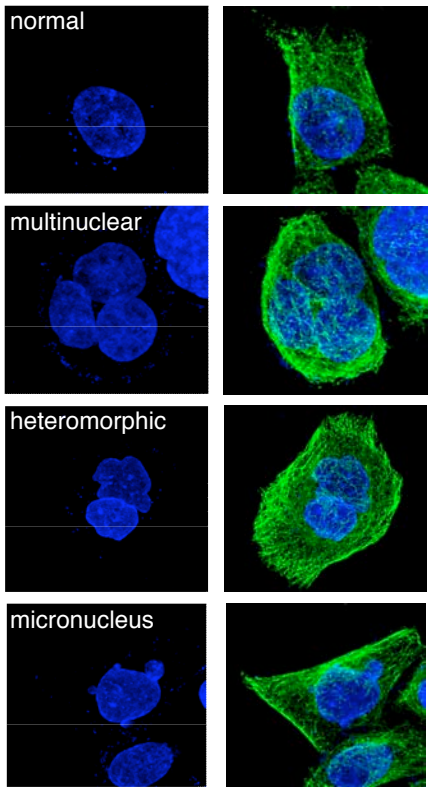


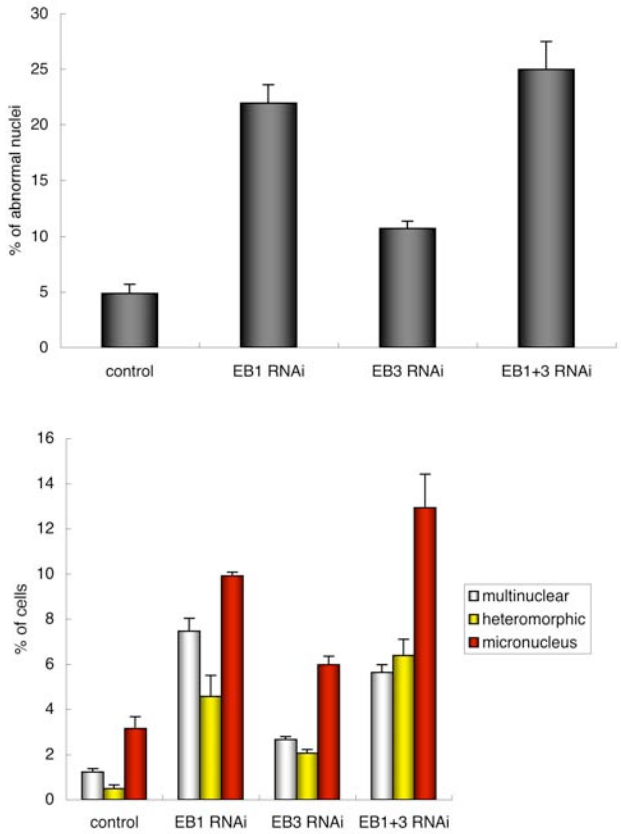

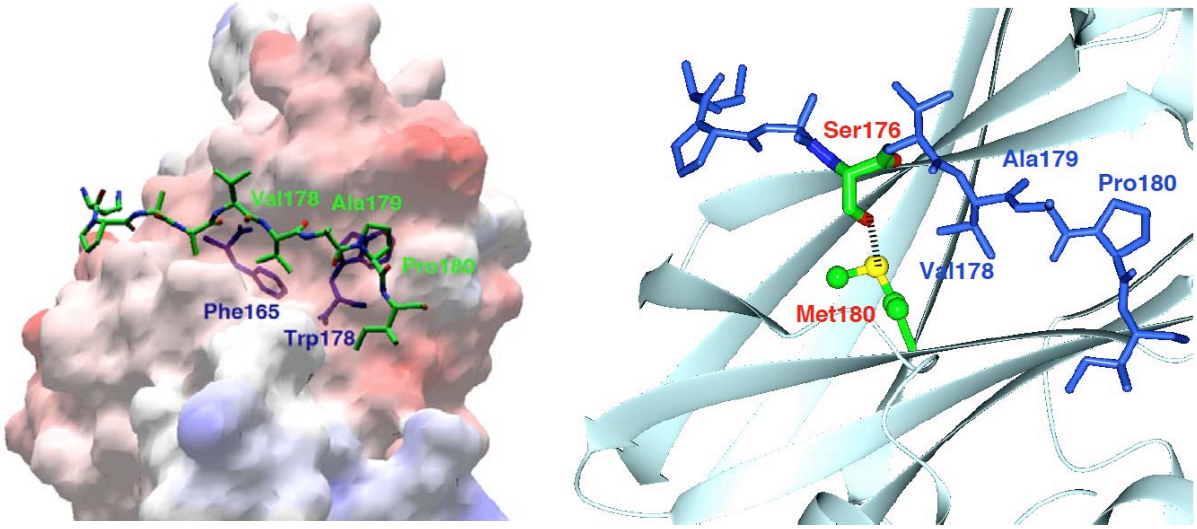


## Supplementary Fig.9

| | | | | | | | | | | | |
|---|---|---|---|---|---|---|---|---|---|---|---|
| | | | | | | V | X | P | | | |
| EB3 | S | G | R | L | S | N | V | A | P | P | C | I |
| NUMB | T | K | P | V | T | V | V | A | P | Q | S | P |
| APC | G | T | V | A | A | R | V | T | P | F | N | Y |
| CBF.1/BOB.1 | N | I | P | C | A | A | V | S | P | N | R | S |
| Synphilin-1 | F | R | P | V | K | R | V | S | P | K | H | Q |
| N-CoR | Q | R | V | S | A | A | V | L | P | L | V | H |
| AF4 | Q | K | P | T | A | Y | V | R | P | M | D | G |
| DCC | T | I | P | T | A | C | V | R | P | T | H | P |
| PHYL | L | R | P | V | A | M | V | R | P | T | V | R |
| VAV | W | F | P | C | N | R | V | K | P | Y | V | H |
| SIP | E | K | P | A | A | V | V | A | P | I | T | T |
| T-STAR | A | R | P | V | G | V | V | V | P | R | G | T |
| Kid | P | L | K | K | A | V | V | M | P | L | Q | L |
| PEG10 | S | P | P | R | A | L | V | L | P | H | I | A |
| DAB-1 | Q | P | P | V | A | Q | V | M | P | G | A | Q |

Supplementary Fig.10

Ban et al.